

Effects of Adiabatic Exponent on Richtmyer–Meshkov Instability *

TIAN Bao-Lin(田保林)** , FU De-Xun(傅德薰), MA Yan-Wen(马延文)

LNM, Institute of Mechanics, Chinese Academy of Sciences, Beijing 100080

(Received 20 May 2004)

We present a systematical numerical study of the effects of adiabatic exponent γ on Richtmyer–Meshkov instability (RMI) driven by cylindrical shock waves, based on the γ model for the multi-component problems and numerical simulation with high-order and high-resolution method for compressible Euler equations. The results show that the RMI of different γ across the interface exhibits different evolution features with the case of single γ . Moreover, the large γ can hold back the development of nonlinear structures, such as spikes and bubbles.

PACS: 47.20.Ma, 47.20.-k, 47.40.-x

Richtmyer–Meshkov instability (RMI) is generated when a shock wave refracts through the interface between two materials.^[1–14] Perturbation on the interface first grows linearly, evolves into nonlinear structures having the form of spikes and bubbles, and then causes the materials to mix. The previous theoretical, experimental and numerical studies of RMI were mainly performed in planar geometry, i.e. driven by planar shock waves. However, in most practical applications, such as inertial confinement fusion (ICF) or supernova, RMI occurs in curved geometry, and the curved geometry complicates the system considerably.

In the past years, research of RMI focused on the effects of Atwood number, shock strength and so on. Moreover, in some numerical simulations, single γ was adopted for the sake of simplicity.^[8,9] In fact, the two materials across the interface are often two different fluids with different γ , more generally, different equations of state. The different equations of state make the model system of RMI considerably complex. Some special phenomena of RMI, such as freezing out or total transmission, can only occur in the case of different γ according to analytic theory.^[3,7]

RMI is closely related to Rayleigh–Taylor instability (RTI) and they share some common features. Livescu *et al.* presented a detailed study of the effects of adiabatic exponent on RTI.^[6] According to the small-amplitude theory for RMI, Yang and Zhang pointed out that the adiabatic exponent affects RMI only in an indirect way, i.e. γ appears as the zeroth-order (unperturbed quantity),^[3] and RMI with smaller γ has larger perturbation growth rate than that with larger γ . Vandenboomgaerde *et al.* presented similar results according to their impulsive model.^[4]

In this Letter, the governing equations of RMI are the two-dimensional compressible Euler equations in cylindrical coordinates, which is convenient for the im-

ploding cylindrical shock waves. Meanwhile, to study the evolution of the instability, we use the level set method^[12] to track the moving interface. Furthermore, to study the effect of different equations of state, we develop a multi-component model, i.e. the γ model, for the compressible RMI problem.^[10] The equation of the model reads

$$\frac{\partial}{\partial t} \frac{1}{\gamma - 1} + u \frac{\partial}{\partial r} \frac{1}{\gamma - 1} + \frac{1}{r} v \frac{\partial}{\partial \theta} \frac{1}{\gamma - 1} = 0, \quad (1)$$

where u and v are the radial and azimuthal velocity components, respectively.

An efficient algorithm is developed to solve the system with both shock waves and contact discontinuities. First, a third-order group velocity control scheme is used to approximate the convective terms,^[11] and the third-order Runge–Kutta method is used to discretize the time derivatives. Secondly, the adaptive grid refinement technique is adopted in the radial direction to improve resolution, and the position of refinement varies with the moving interface. Thus all the above-mentioned methods compose the high-order high-resolution numerical methods for the RMI in the present study.

As for the physical parameters used here, the radius and the velocity are normalized by the mean radius of the material interface and the speed of the incident shock at $t = 0$, similar to Ref. [5]. The interface locates initially at $r = 1 + a_0 \sin(k\phi)$, where a_0 is the dimensionless initial perturbation amplitude and k is the wave number. In the simulation, the incident shock Mach number is 1.22 with $a_0 = 0.033$ and $k = 12$. The initial configuration is also shown in Fig. 1, where the imploding shock, interface and two fluids are marked schematically.

In the following, we give some simulation results of one or two γ across the material interface with the initial density ratio equal to 7.25 for all the cases. The

* Supported in part by the National Natural Science Foundation of China under Grant Nos 10176033 and 90205025, the Special Funds for Major State Basic Research Project of China under Grant No G1999032805, and the National High-Tech ICF Committee of China.

** Email: tianbl@lnm.imech.ac.cn

©2004 Chinese Physical Society and IOP Publishing Ltd

incident imploding shock travels from an outer heavy fluid to inner light fluid. When colliding with the interface, the shock wave bifurcates into a transmitted one and a rarefaction wave. The phenomenon of phase inversion occurs immediately, i.e. the initial crests and troughs of the perturbed interface exchange their positions in the phase inversion stage. Then the perturbation at the interface continues to develop asymmetrically, which results in complex nonlinear structures finally.

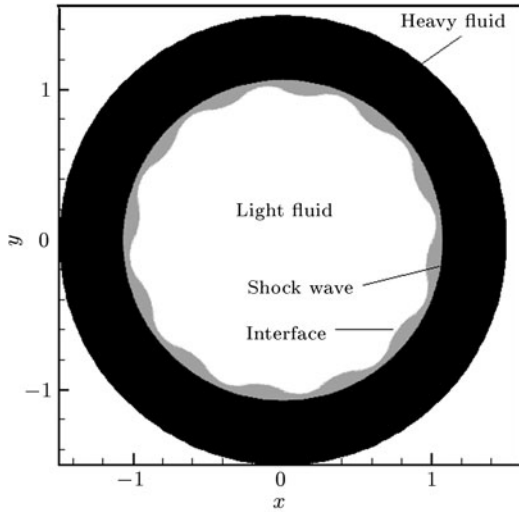


Fig. 1. Initial value distribution.

Firstly, we examine the case with the same γ across the interface. The nonlinear structures of bubble and spike appear as shown in Fig. 2 at $t = 3.0$ with $\gamma = 1.4$ and 2.1 respectively. We can see that in the case of large γ , the spikes become short and narrow, whereas the difference is not very apparent. As we know, γ is an important physical parameter of the compressibility of ideal gases. According to the relation of normal shock, we know that the compressible limit of ideal gases is $(\gamma + 1)/(\gamma - 1)$, so the larger the γ value of a gas, the harder the gas can be compressed. The averaged interface position shown in Fig. 3 implies how much the inner fluid can be compressed.

Secondly, when two different γ across the material interface are adopted, the interface structures exhibit quite different features to the cases of single γ . For the cases of inner fluid with smaller γ than outer one, i.e. Fig. 4(a), the spikes are spear-like and penetrate into the light fluid more deeply, and the bubbles are slightly narrower than that in a single γ . Moreover, the roll-up of spikes is not manifest. However, in the cases of inner fluid with larger γ , i.e. Fig. 4(b), the development of nonlinear structures of the spikes and bubbles is restrained to some extent, and the roll-up of the spikes is more manifest.

In fact, for the cases with smaller γ of inner fluid, the outer fluid seems to be harder, while the inner one

seems to be softer due to different compressibilities of the different γ . Thus the spikes can penetrate into the light fluid more deeply. For the case as shown in Fig. 4(b) and γ ($\gamma_{\text{outer}} = 1.4$, $\gamma_{\text{inner}} = 1.67$), the situation is just opposite to the case of $\gamma_{\text{outer}} = 1.4$ and $\gamma_{\text{inner}} = 1.26$ [Fig. 4(a)].

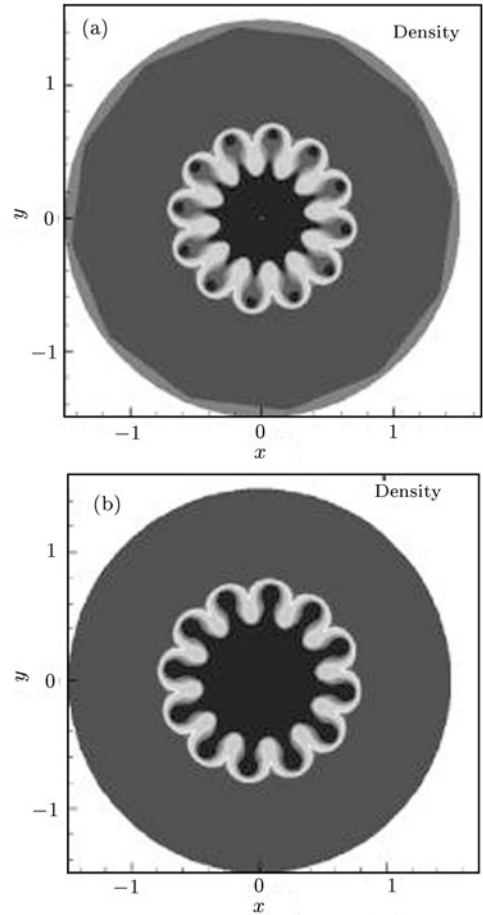


Fig. 2. Density contours (a) at $t = 3.0$ and $\gamma = 1.4$ and (b) at $t = 3.0$ and $\gamma = 2.1$.

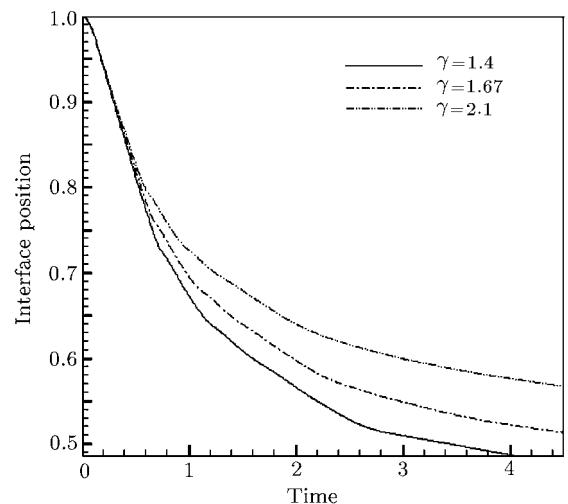


Fig. 3. Averaged interface position versus time with different γ .

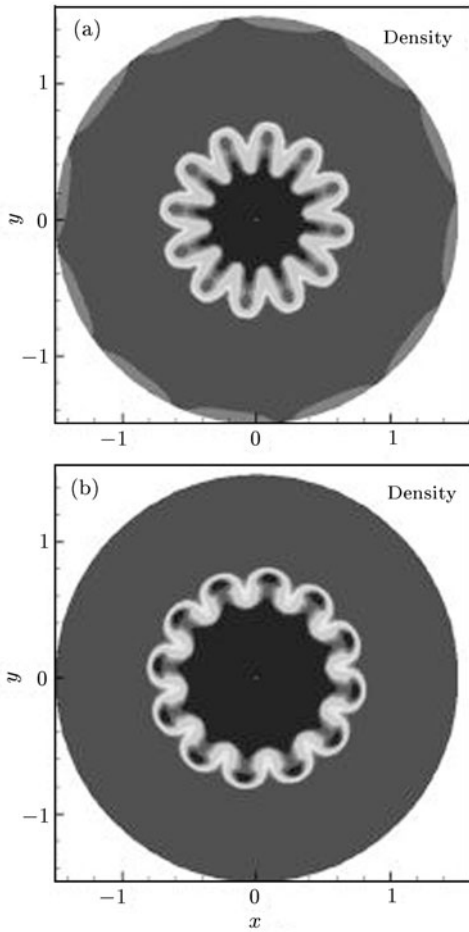


Fig. 4. Density contours (a) $\gamma_{\text{outer}} = 1.4$ and $\gamma_{\text{inner}} = 1.26$ and (b) $\gamma_{\text{outer}} = 1.4$ and $\gamma_{\text{inner}} = 1.67$, at $t = 3.0$.

Figure 5 shows the time evolution of the perturbation amplitude and the growth rate with different γ distributions. Here the perturbation amplitude is defined as

$$a = \frac{1}{2}(r_{\text{max}} - r_{\text{min}}), \quad (2)$$

where r_{max} and r_{min} are the maximum and minimum radius of interface respectively, and the growth rate is the derivative of the perturbation amplitude with respect to time. We can see that the cases of γ ($\gamma_{\text{outer}} = 1.4$ and $\gamma_{\text{inner}} = 1.26$) and γ ($\gamma_{\text{outer}} = 1.4$ and $\gamma_{\text{inner}} = 1.4$) are similar, while the case of γ ($\gamma_{\text{outer}} = 1.4$ and $\gamma_{\text{inner}} = 1.67$) is quite different from the other two cases. At early time, the discrepancy of the three cases is small, but at late time the results of the case of $\gamma_{\text{outer}} = 1.4$ and $\gamma_{\text{inner}} = 1.67$ are clearly discrepant to the other two. At late time, the shock strength becomes very weak, so it is difficult to compress the inner fluid with large γ . Thus the perturbation amplitude and growth rate of γ ($\gamma_{\text{outer}} = 1.4$ and $\gamma_{\text{inner}} = 1.67$) are smaller than those of other two cases.

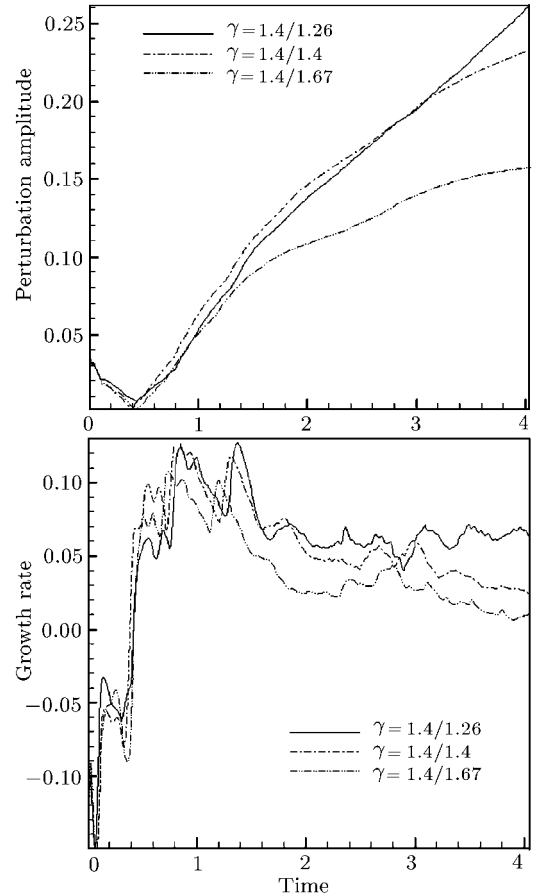


Fig. 5. (a) Perturbation amplitude and (b) perturbation growth rate versus time.

In summary, the adiabatic exponent plays an important part in the evolution of the interface. The effects of different adiabatic exponents have been studied by using the γ model for multi-component problems and the high-order high-resolution method for the compressible Euler equations. In the cases with different γ , the interface structures are quite different from the cases with single γ . A large γ of the inner fluid can limit the development of the spikes and bubbles due to the different compressibilities of the ideal gases with different γ .

References

- [1] Richtmyer R D 1960 *Commun. Pure Appl. Math.* **13** 297
- [2] Meshkov E E 1970 *NASA Tech. Trans. F* **13** 074
- [3] Yang Y and Zhang Q 1994 *Phys. Fluids* **6** 1856
- [4] Vandenboomgaerde M et al 1998 *Phys. Rev. E* **58** 1874
- [5] Zhang Q 1998 *Phys. Fluids* **10** 974
- [6] Livescu D 2004 *Phys. Fluids* **118** 974
- [7] Mikaelian K Q 1994 *Phys. Fluids* **6** 356
- [8] Cohen R H et al 2003 *Phys. Fluids* **14** 3691
- [9] Zabusky N J et al 2003 *J. Fluid Mech.* **475** 147
- [10] Shyue K M 1998 *J. Comput. Phys.* **142** 208
- [11] Tian B L et al 2004 *Chin. J. Comput. Mech.* (at press)
- [12] Sethian J A et al 2003 *Ann. Rev. Fluid Mech.* **35** 341
- [13] Ling G C and Zhao H L 2003 *Chin. Phys. Lett.* **20** 383
- [14] Tang Z M and Hu W R 2003 *Chin. Phys. Lett.* **20** 526